

Published in final edited form as:

Nat Commun. ; 6: 8431. doi:10.1038/ncomms9431.

## The hand of *Homo naledi*

Tracy L. Kivell<sup>1,2,3</sup>, Andrew S. Deane<sup>4,3</sup>, Matthew W. Tocheri<sup>5,6</sup>, Caley M. Orr<sup>7</sup>, Peter Schmid<sup>8,3</sup>, John Hawks<sup>9,3</sup>, Lee R. Berger<sup>3</sup>, and Steven E. Churchill<sup>10,3</sup>

<sup>1</sup>Animal Postcranial Evolution Lab, Skeletal Biology Research Centre, School of Anthropology and Conservation, Marlowe Building, University of Kent, Canterbury CT2 7NR United Kingdom

<sup>2</sup>Department of Human Evolution, Max Planck Institute for Evolutionary Anthropology, Deutscher Platz 6, 04103 Leipzig, Germany <sup>3</sup>Evolutionary Studies Institute and Centre for Excellence in Palaeosciences, University of the Witwatersrand, Private Bag 3, Wits 2050, South Africa

<sup>4</sup>Department of Anatomy and Neurobiology, College of Medicine, University of Kentucky, MN 224

UK Medical Centre, Lexington KY, USA 40536-0098 <sup>5</sup>Department of Anthropology, Lakehead

University, Thunder Bay ON P7K 1L8, Canada <sup>6</sup>Human Origins Program, Department of Anthropology, National Museum of Natural History, Smithsonian Institution, Washington, DC

20560, USA <sup>7</sup>Department of Cell and Developmental Biology, University of Colorado School of

Medicine, Aurora, CO 80045, USA <sup>8</sup>Anthropological Institute and Museum, University of Zuerich,

Winterthurerstr. 190, CH-8057 Zuerich, Switzerland <sup>9</sup>Department of Anthropology, University of

Wisconsin-Madison, Madison, WI 53593 USA <sup>10</sup>Department of Evolutionary Anthropology, Duke

University, Box 90383 Durham NC, USA 27708-9976

### Abstract

A nearly complete right hand of an adult hominin was recovered from the Rising Star cave system, South Africa. Based on associated hominin material, the bones of this hand are attributed to *Homo naledi*. This hand reveals a long, robust thumb and derived wrist morphology that is shared with Neandertals and modern humans and considered adaptive for intensified manual manipulation. However, the finger bones are longer and more curved than in most australopiths, indicating frequent use of the hand during life for strong grasping during locomotor climbing and suspension. These markedly curved digits in combination with an otherwise human-like wrist and palm indicate a significant degree of climbing, despite the derived nature of many aspects of the hand and other regions of the postcranial skeleton in *H. naledi*.

---

Users may view, print, copy, and download text and data-mine the content in such documents, for the purposes of academic research, subject always to the full Conditions of use:[http://www.nature.com/authors/editorial\\_policies/license.html#terms](http://www.nature.com/authors/editorial_policies/license.html#terms)

Corresponding author: T. L. K. (t.l.kivell@kent.ac.uk).

#### Author Contributions

L.R.B., S.E.C., P.S. and J.H. conceived the project. T.L.K. conducted linear analyses. A.S.D. performed phalangeal curvature analyses and surface scanning. M.W.T. and C.M.O. conducted 3D analyses of wrist bones. P.S. composed composite image of hand bones. T.L.K, M.W.T., C.M.O., A.S.D and S.E.C. wrote the paper.

#### Additional Information

**Supplementary Information** accompanies this paper at [www.nature.com/naturecommunications](http://www.nature.com/naturecommunications)

**Competing financial interests:** The authors declare no competing financial interests.

A longstanding palaeoanthropological debate concerns the degree to which arboreal climbing and suspension remained an important component of the early hominin behavioural repertoire. Hominin hand anatomy can provide valuable insights into this debate, but well-preserved hand bones are relatively rare in the fossil record, and multiple hand bones from the same individual are even rarer. To date, nearly 150 hand bone specimens attributed to *H. naledi*<sup>1</sup> have been uncovered from the Dinaledi Chamber of the Rising Star cave system<sup>2</sup>, representing at least six adults and two immature individuals. Twenty-six of these bones are from the right hand (Hand 1) of an adult individual. Missing only its pisiform (postmortem), this hand is part of the paratype of *H. naledi* and was recovered partially articulated with the palm up and fingers flexed (Fig. 1). This hand is small, similar in size to that of the *Australopithecus sediba* female MH2<sup>3</sup>, although there are other adult hand bones in the *H. naledi* sample that are slightly smaller and others slightly larger<sup>1</sup> Here we focus on the comparative and functional morphology of this nearly complete hand.

Our comparative analyses reveal that the wrist and palm are generally most similar to those of Neandertals and modern humans, while the fingers are more curved than some australopiths. This distinctive mosaic of morphology has yet to be observed in any other hominin taxon, and suggests use of the hand for arboreal locomotion in combination with forceful precision manipulation typically used during tool-related behaviours.

## Results

### The thumb

Modern humans and archaic humans (as represented here by Neandertals) differ from other apes in having short fingers relative to a long and robust thumb with well-developed thenar musculature that facilitates forceful precision and precision-pinch grips between the thumb and fingers<sup>4-6</sup>. Most australopiths (e.g., *Australopithecus afarensis* and *Australopithecus africanus*) have thumb-finger length proportions estimated to be similar to humans<sup>7-9</sup> (but see<sup>10</sup>), but with gracile pollical metacarpals (Mc1) that lack strong muscle attachments<sup>11,12</sup>. The almost complete hand of *Au. sediba* MH2 has a gracile but remarkably long thumb, outside the range of variation in recent humans<sup>3</sup>. Hand 1 also has a long thumb: the first ray length (Mc1 + PP1 = 61.9 mm) is 58% of the third (Mc3 + PP3 + IP3 = 107.5 mm), falling only within the upper range of variation in modern human males (mean 55%) and outside the female range of variation (mean 54%; Fig. 2). The curvatures of the pollical carpometacarpal articulation fall within the modern human range of variation, unlike the more curved facets of extant great apes and some other early hominins<sup>13</sup>. Unlike most australopiths, Hand 1, as well as six additional Mc1 specimens from five other individuals, demonstrate that *H. naledi* has markedly robust pollical metacarpals with well-developed crests for the opponens pollicis and the first dorsal interosseous muscles (Fig. 3 and Supplementary Fig. 1, Supplementary Table 1 and Supplementary Note 1). The former muscle is functionally important for opposition of the thumb to the fingers as well as holding and manipulating large objects, while the latter muscle is strongly recruited during precision and precision-pinch grips<sup>14</sup>. In *H. naledi*, the flaring crests on the Mc1 for the intrinsic thenar muscles are accompanied by a prominent palmar ridge running sagittally along the

midshaft (Fig. 3). Overall, the well-developed thenar muscle attachments are most similar to those seen in modern humans, Neandertals and the Swartkrans pollical metacarpals [SK 84 and SKX 5020, attributed to either *Au. (Paranthropus) robustus* or early *Homo*]<sup>15-17</sup>. In contrast, they are unlike the weakly-developed muscle attachments of gracile australopiths<sup>3,11,12</sup> and *Ardipithecus ramidus*<sup>18</sup>.

Notwithstanding these similarities to modern humans and Neandertals, other aspects of the thumb morphology of *H. naledi* differ from these taxa in interesting ways. The base and proximal articular facet of the pollical metacarpal are remarkably small relative to its length both radioulnarly and dorsopalmarly in Hand 1 and in the six additional pollical metacarpals from Dinaledi (Fig. 3 and Supplementary Fig. 1). The distal articular surface is also dorsopalmarly flat compared with other hominins and strongly asymmetric with a much larger palmar-radial protuberance. The *H. naledi* pollical distal phalanx (n=2) is large and robust; its apical tuft is radioulnarly broader relative to its length than those of australopiths, SKX 5016, Neandertals, and modern humans (Fig. 1; Supplementary Table 2). Its overall shape and apical tuft breadth most resemble the morphology of *Homo habilis* OH7 and *Au. robustus* TM 1517k; however, unlike OH7, *H. naledi* demonstrates a well-developed ridge along the distal border of a deep proximal palmar fossa for the attachment of flexor pollicis longus tendon. The radial and ulnar tips of the apical tuft project proximopalmarly as ungual spines and there is a distinct area for the ungual fossa. Some of these features are found in early hominins<sup>18-20</sup>, but the full suite of features in *H. naledi* suggests it had a well-developed flexor pollicis longus muscle and a very broad, human-like palmar pad with a mobile proximal pulp<sup>19,21</sup>. These features facilitate forceful pad-to-pad gripping between the thumb and fingers<sup>5,21</sup>. The non-pollical distal phalanges corroborate this functional interpretation, being robust like that of Neandertals<sup>17,22,23</sup> and more radioulnarly expanded than all australopiths and modern humans (Fig. 1 and Supplementary Table 2).

## The wrist

The robust pollical metacarpals of modern humans and Neandertals are associated with a suite of changes in carpal bone shape and articular configuration compared with extant great apes. These changes include a large Mc1 facet on the trapezium, a relatively large trapezium-scaphoid joint that extends onto the scaphoid tubercle, a boot-shaped trapezoid with an expanded palmar surface, a relatively large and more palmarly-placed capitate-trapezoid articulation, and the shift of a separate ossification centre from the capitate to the base of the Mc3 that results in a styloid process<sup>5,13,24,25</sup>. In addition, the Mc2 articulations with the trapezium and capitate are more proximodistally oriented, which acts to keep the trapezium-trapezoid and capitate-trapezoid joints in maximum contact during forceful precision and power grips<sup>5,25,26</sup>. Altogether, this derived complex of pollical and radial wrist features likely functions to distribute compressive loads and minimize shear during strong precision and precision-pinch grips involving the robust thumb and thenar musculature<sup>13,25,27</sup>.

Although some fossil hominins (e.g., australopiths, OH7) variably share one or more of these features with modern humans and Neandertals, others (e.g., *Homo floresiensis*) do not share any<sup>11,28-33</sup>. Overall no early hominin taxon shows conclusive evidence that it had the

full morphological complex or even a majority of the modern human features within it<sup>13,32-34</sup>. However, the absence of fossil wrist bones attributed to *Homo erectus sensu lato*, apart from a partial lunate<sup>35</sup>, complicates evolutionary interpretations of this anatomical region. The presence of a human-like styloid process on a Mc3 from Kaitio, Kenya (KNM-WT 51260), dated to ~1.42 Ma and plausibly attributed to *H. erectus s. l.*, is the only evidence suggesting that this complex may have arisen early in the evolution of the genus *Homo*<sup>26</sup>.

In this context, the almost complete right wrist of Hand 1 provides a rare opportunity to examine this suite of carpal features in its entirety from a single fossil hominin individual (Figs. 1 and 4). Comparative 3D morphometric analyses of the scaphoid, trapezium and trapezoid (Fig. 5a and Supplementary Table 3a), and the capitate and hamate (Fig. 5b and Supplementary Table 3b) demonstrate that *H. naledi* wrist shape and articular configuration fall well within the ranges of variation seen in modern humans and Neandertals and are thus derived relative to extant great apes, australopiths and *H. floresiensis*. Hand 1 and several other isolated carpal bones (Supplementary Table 1), have a relatively flat trapeziometacarpal joint, a facet for the trapezium that extends onto the scaphoid tubercle, an enlarged and palmarly-expanded trapezoid-capitate joint, and a boot-shaped trapezoid with an expanded palmar nonarticular surface that probably repositions the thumb into a more supinated position compared with australopiths, OH7 and *H. floresiensis*<sup>32,34</sup>. Although the tubercle of the trapezium and the hamulus of the hamate are robust, both fall within the range of variation documented in modern humans and Neandertals (Fig. 4 and Supplementary Fig. 2).

However, some features in *H. naledi* fall near the edge or outside the ranges of variation observed in modern humans/Neandertals. Most striking are the small relative sizes of the trapezium's Mc1 and scaphoid facets (12.3% and 6.6% of total trapezium area, respectively), which parallel the noticeably small Mc1 base and trapezoid facet<sup>36</sup>. The angle between the capitate's second and third metacarpal facets of Hand 1 (108°) is also lower than that of any modern human (mean 140° ± 9°) or Neandertal (mean 132° ± 9°) in our sample (n=82), and is more similar to that seen in some australopiths and *H. floresiensis*<sup>32,33</sup> (Supplementary Fig. 3). Finally, the *H. naledi* third metacarpal (n=3) lacks a styloid process, suggesting that the Mc3 styloid may not have arisen within the genus *Homo* as part of an evolutionarily integrated complex of radial carpometacarpal features. These specific morphological distinctions from the typical conditions observed in modern humans and Neandertals, however, do not detract from the otherwise overall similarity in carpal shape and articular configuration shared by Hand 1, modern humans, and Neandertals (Figs. 4 and 5). In conjunction with a robust and relatively long thumb, our results suggest that *H. naledi*, Neandertals, and modern humans share a derived complex of features in the radial wrist and distal carpal row that distinguishes them from other early hominin taxa<sup>25,32-34</sup>.

### The non-pollical metacarpals

Modern human and Neandertal non-pollical metacarpals (Mc2-Mc5) differ from extant great apes in being relatively short and robust with asymmetrical head morphology (particularly that of the Mc2 and Mc5), and a saddle-shaped Mc5-hamate joint, all of which facilitate

pad-to-pad contact between the fingers and thumb<sup>5,17,34,37</sup>. These features are absent in *Ar. ramidus*<sup>18</sup>, but most australopiths display derived, short, robust metacarpals with asymmetrical heads<sup>3,7,11,12</sup>. The Hand 1 metacarpals are generally similar in overall robusticity to most australopiths, Neandertals and modern humans, and do not have the unusually radioulnarly-narrow metacarpal shafts typical of *Au. sediba* MH2<sup>3</sup> (Fig. 6 and Supplementary Figs. 4-6). The *H. naledi* Mc5 (n=2) is particularly robust, like that of *Au. africanus* (StW 63) and Swartkrans SK(W) 14147, with a well-developed crest for the opponens digiti minimi muscle (Supplementary Fig. 6). However, unlike australopiths and the Swartkrans specimens, *H. naledi* shares with modern humans a mildly saddle-shaped Mc5-hamate articulation, which facilitates rotation of the fifth digit toward the thumb and index finger<sup>22,37</sup>. Overall, *H. naledi*, Neandertals and modern humans share metacarpal morphology that is consistent with an enhanced and derived ability to cup and manipulate objects within one hand relative to extant great apes<sup>5,37</sup>.

### The phalanges

Modern human and Neandertal proximal and intermediate phalanges are shorter, less curved, and less robust, with poorly-developed flexor tendon attachments compared with those of extant great apes (Fig. 7). Australopiths and OH7 generally demonstrate an intermediate condition, being slightly longer, more curved, and/or more robust than the typical modern human/Neandertal morphology, but less so than observed in the extant apes<sup>11,12,28,31,38</sup>.

In comparison with the generally modern human/Neandertal-like morphology of the *H. naledi* wrist, thumb and palm, the fingers of Hand 1 are long and remarkably curved, similar to those of extant apes and early hominins (Fig. 7 and Supplementary Fig. 7 and Supplementary Table 4). The mean curvature of *H. naledi* proximal phalanges (PP, n=11) is almost identical to that of *Au. afarensis* and OH7, and is not statistically distinct from African apes. The mean curvature of the intermediate phalanges (IP, n=14) is higher than that of any other hominin and not statistically distinct from Asian apes (Fig. 7). Although there is variation across fossil hominins, a combination of both highly curved PPs and IPs is unusual; extant apes and most fossil hominins, such as *Au. afarensis* and OH7, generally have more strongly curved PPs and comparatively straight IPs. Experimental, behavioural and morphological evidence has demonstrated that phalangeal curvature is an adaptive response to the habitual stresses of locomotion, with more arboreal primates, especially those that often engage in suspension or climbing, having stronger longitudinal curvature compared with more terrestrial primates<sup>38-44</sup>. Biomechanically, curvature reduces the overall strain experienced by the phalanx during flexed-finger grasping postures because a curved bone is more closely aligned with the joint reaction forces<sup>42,44</sup>. Thus, the strong degree of phalangeal curvature in *H. naledi* is a clear functional indication that its fingers experienced high loads during grasping required for climbing or suspensory locomotion. Furthermore, the degree of phalangeal curvature has been shown to respond to mechanical loading throughout ontogeny; primates that are more arboreal as juveniles than as adults show less curvature in adulthood<sup>45</sup>. The *H. naledi* sample includes one immature PP (UW 101-1635) and its curvature is less than that of the *H. naledi* adult mean, but within the low range of the adult variation (Fig. 7). This ontogenetic evidence suggests that *H. naledi* adults

were using their hands for climbing during life just as much, if not more so, than the juveniles.

Hand 1 also has relatively long fingers. Relative finger-to-palm proportions vary strongly across fossil hominins and across different rays within individual hands (Supplementary Fig. 7). However, Hand 1 has longer third and fourth digits (PP length alone or PP + IP length/metacarpal length) than all other fossil hominins except *Ar. ramidus* and the early modern human Qafzeh 9 (the latter with unusually long, but comparatively straight, phalanges). Hand 1 intermediate phalanges are proportionately longer than those of australopiths and most later *Homo* individuals and have a well-developed median bar indicative of high loading<sup>46</sup>. Long and curved fingers are consistent with the functional interpretation that *H. naledi* was using its hand for locomotor grasping. However, the phalangeal flexor sheath ridges on the PPs are not well-developed and are most similar in overall shape and robusticity to those of modern humans (Supplementary Fig. 8). Such morphology is consistent with the generally gracile morphology of the upper limb<sup>1</sup>, and may also be a biomechanical consequence of strong phalangeal curvature<sup>44</sup>. Overall, the remarkable curvature of both the PPs and IPs unambiguously indicates that locomotor grasping during climbing or suspension was a significant component of the *H. naledi* behavioural repertoire.

## Discussion

Over the course of human evolution, the hand was freed from the constraints of locomotion and has evolved primarily for manipulation. However, reconstructing the hands' transition to bipedality and to tool-use has been the source of much debate<sup>5,6,34,37,47</sup>. Furthermore, the few hand bones attributed to *H. erectus s.l.*<sup>22,26,35</sup> are not an adequate sample from which to confidently test hypotheses about the evolution of the hominin wrist and hand during this transitional period. Australopiths and *H. habilis* are characterised by derived, human-like morphologies, primarily of the lower limb, that clearly indicate habitual bipedalism, but also varying suites of primitive, great ape-like features, primarily of the upper limb, that have elicited different functional interpretations. Some view the primitive features of early hominins as retentions from an arboreal ancestor that were either being lost or were selectively neutral and, as such, considered largely non-functional and adaptively insignificant<sup>48</sup>. Others, who aim to reconstruct early hominin behaviour as a whole, consider the primitive features as functionally useful with adaptive value retained under stabilizing selection<sup>49,50</sup>. Resolution of this debate requires morphological features that are ontogenetically sensitive to loading during life and, as such, can demonstrate how a bone was used during an individual's lifetime<sup>51</sup>.

The strongly curved phalanges of *H. naledi* in association with an otherwise modern human/Neandertal-like hand, provide key evidence, consistent with primitive morphologies of the upper limb and thorax<sup>1</sup>, for the retention of a significant frequency of climbing in a fossil hominin biped<sup>1,52</sup> that was also apparently adapted to the demands of intensified manipulative behaviours. The curvature of other early hominin (i.e., australopiths and OH7) phalanges is intermediate between that of extant apes and modern humans, and it has been argued that these curved digits indicate frequent use of arboreal substrates in these hominins<sup>49,50</sup>. In contrast to the phalangeal morphology, the full suite of derived thumb and

wrist features in Hand 1 is found only in committed, habitual tool-users (e.g., Neandertals and modern humans), suggesting that much of the hand anatomy in *H. naledi* may be the result of selection for precision handling and better distribution of compressive loads during forceful manipulative behaviours such as tool-making and tool-use (although tools have not been recovered in the Dinaledi Chamber itself<sup>2</sup>). Nevertheless, long and curved phalanges clearly suggest use of the hand during life for powerful locomotor grasping and the functional importance of climbing in *H. naledi*. Therefore, as a whole, Hand 1 demonstrates that the ability for forceful precision manipulation is compatible with use of the hand for arboreal locomotion. Whether or not this dual role required functional trade-offs that compromised the performance of these behaviors to some degree is currently unclear. When further considered within the context of the human-like foot<sup>52</sup> and long lower limb<sup>1</sup> in *H. naledi*, the hand morphology is consistent with the hypothesis that early hominins retained primitive use of the upper limb, even while fine-tuning specific aspects of the postcranial anatomy to facilitate novel behaviours such as efficient terrestrial locomotion and tool use.

## Methods

### Comparative morphometric analysis

*H. naledi* hand remains were compared with the morphology of the original fossils of *Ar. ramidus*, *Au. afarensis*, *Au. africanus*, *Au. sediba*, *Au. robustus*/early *Homo* from Swartkrans, *H. habilis*, *H. neanderthalensis*, and early modern *H. sapiens*. Metric data were also compared to published data on *H. neanderthalensis* from Shanidar<sup>17</sup>, Krapina and Kiik-Koba<sup>53</sup>. The composite hand of *Au. afarensis*, used to determine the estimated relative thumb length, includes the following specimens: AL333w-39 (Mc1), AL333-69 (PP1), AL333-16 (Mc3), AL333-63 (PP3), AL333-88 (IP3), following Marzke<sup>7</sup>. The extant comparative sample included *Pan troglodytes*, *P. paniscus*, *Gorilla gorilla*, *G. berengei* and modern humans. The modern human sample comprised Nubian Egyptians, Europeans, Africans, small-bodied Khoisan, and skeletally-robust Tierra del Fuegians. Samples of extant taxa and specimens for fossil taxa varied depending on the analyses; thus, this information is provided for each analysis in the Supplementary Information.

Standard length and breadth measures of the metacarpals and phalanges were compared across the extant and fossil samples using box-and-whisker plots (Supplementary Figs. 1, 4-8). Metacarpal measurements included total and interarticular proximodistal length of the bone, maximum radioulnar breadth of the proximal and distal articular surfaces, and maximum radioulnar breadth of the proximal, mid- and distal shaft. Phalangeal measurements included total length and maximum radioulnar breadth of the proximal end, midshaft and trochlea.

### Multivariate analyses of 3D models

3D surface models of carpal bones were generated using laser and CT scanning, following procedures outlined elsewhere (see Tocheri et al.<sup>54</sup> and references therein) The articular and nonarticular areas of each carpal bone were segmented using Geomagic Studio software, typically while using the actual bone as a reference. Scale-free metrics that capture different aspects of carpal shape were then quantified<sup>55-57</sup>. These metrics include curvatures

(radioulnar and dorsopalmar) of the first metacarpal facet on the trapezium, relative areas of articular and nonarticular surfaces, and angles between articular surfaces (see<sup>13,25,58,59</sup> for further methodological details on these methods). These data were analyzed using canonical variates (CVA) and linear discriminant function (DFA) analyses to examine the overall morphometric similarities and differences among extant and fossil hominid taxa (Fig. 5). In the scaphoid-trapezium-trapezoid analysis (Fig. 5A), sample sizes were as follows: 106 modern humans, 65 *Pan*, 57 *Gorilla*, 8 *Pongo*, 1 Neandertal, and 1 *H. naledi*; in the capitate-hamate analysis (Fig. 5B), sample sizes were as follows: 62 modern humans, 40 *Pan*, 18 *Gorilla*, 16 *Pongo*, 3 Neandertals, 1 *H. floresiensis*, 1 *Au. sediba*, 2 *Au. afarensis*, and 1 *H. naledi*.

### High-resolution polynomial curve fitting methodology

All phalangeal curvatures were quantified using high-resolution polynomial curve fitting (HR-PCF) methods<sup>38,43,60</sup>. Although HR-PCF analysis is not software dependent, all curvatures were quantified using proprietary HR-PCF curve fitting software<sup>43</sup>. Unlike traditional curvature quantification techniques (i.e., included angle, normalized curvature moment arm) that model curvature as an imaginary line passing through the center of a bone, HR-PCF models the surface curvature of the bone and can fit a polynomial function to either the dorsal or palmar surface of a phalanx. The palmar surfaces of many phalanges were interrupted by flexor sheath ridges that create irregularities in the outline of shaft curvature, so the more regular dorsal margin of the outline was chosen for polynomial fitting. Although it could be argued that the dorsal and palmar curvatures are responses to different loading regimes, they are highly interdependent and associated with the same positional behavior.

Elements were photographed in a lateral and standardized orientation. JASC PSP image editing software was used to convert the resulting 2D images into simple digitized outlines. These digitized outlines contain thousands of individual pixels, each having its own paired co-ordinates. End points were selected for each dorsal contour to represent the limits of a discrete 2nd order curve and the co-ordinates of the individual pixels comprising the selected portion of the dorsal contour were used as data points to generate a best-fit 2nd order polynomial function with three coefficients defined as  $y = Ax^2 + Bx + C$ . The three resulting co-efficients (A,B,C) can be used as the raw data in a statistical analysis. The first coefficient (A) expresses the nature and degree of the longitudinal curvature whereas the second (B) and third (C) reflect aspects of the orientation of that curve with respect to the rest of the element (i.e., element rotation, element position in 2D space). Given the limitations of coefficients B and C to represent meaningful information about the magnitude of phalangeal shaft curvature, only the 1st (A) polynomial coefficient was considered in statistical analyses performed in the present study.

Although any order of polynomial can be used with HR-PCF methods, a 2nd order polynomial was chosen over a higher-order polynomial functions because 2nd order curves (e.g., longitudinal phalangeal shaft curvature) have no structural points of inflection, unlike 3rd order curves and above, which impose either one or more points of inflection. The coefficients of higher-order polynomials (i.e., 3rd–6th order) are very sensitive to whatever



irregularities exist in the contours of anatomical curves. A more detailed treatment of the HR-PCF method is presented in Deane et al.<sup>43</sup>.

The mean curvatures for discrete taxonomic samples were compared directly using a One-Way ANOVA with a Bonferroni correction.

## Supplementary Material

Refer to Web version on PubMed Central for supplementary material.

## Acknowledgements

We thank the National Geographic Society and the National Research Foundation for particularly significant funding of both the discovery, recovery and analysis of this material. We thank the University of the Witwatersrand and the Evolutionary Studies Institute as well as the South African National Centre of Excellence in Palaeosciences for curating the material and hosting the authors while studying the material. We thank S. Potze, L.C. Kgasi and the Ditsong National Museum of Natural History, B. Zipfel and the University of the Witwatersrand, Y. Rak, I. Hershkovitz and Tel Aviv University, T. White, W. Kimbel, B. Asfaw, G. Semishaw, Y. Assefa, G. Shimelies and National Museum of Ethiopia, A. Gidna, A. P. Kweka and Museum and House of Culture Tanzania for access to comparative fossil collections; curators at Museum für Naturkunde Berlin, Max-Planck-Institut für evolutionäre Anthropologie, Naturhistorisches Museum Wien, Universität Wien, Musée royal de L'Afrique central, Università degli Studi di Firenze and the Powell Cotton Museum for access to comparative extant material; S. Traynor for help with photography. Partial funding for aspects of this research was provided by the European Research Council Starting Grant #336301 (T.L.K.), the Max Planck Society (T.L.K.) and the Smithsonian Scholarly Studies Program (M.W.T.).

## References

- Berger LR, et al. A new species of the Genus *Homo* from the Dinaledi Chamber, South Africa. *Elife* in press.
- Berger LR, et al. Geological and taphonomic evidence for deliberate body disposal by the primitive hominin species *Homo naledi* from the Dinaledi Chamber, South Africa. *ELife* in press.
- Kivell TL, Kibii JM, Churchill SE, Schmid P, Berger LR. *Australopithecus sediba* hand demonstrates mosaic evolution of locomotor and manipulative abilities. *Science*. 2011; 333:1411–1417. [PubMed: 21903806]
- Napier, JR. *Hands*. Princeton University Press; Princeton: 1993.
- Marzke MW. Precision grips, hand morphology and tools. *Am. J. Phys. Anthropol.* 1997; 102:91–110. [PubMed: 9034041]
- Susman RL. Hand function and tool behaviour in early hominids. *J. Hum. Evol.* 1998; 35:23–46. [PubMed: 9680465]
- Marzke MW. Joint functions and grips of the *Australopithecus afarensis* hand, with special reference to the region of the capitate. *J. Hum. Evol.* 1983; 12:197.
- Alba DM, Moyà-Solà S, Köhler M. Morphological affinities of the *Australopithecus afarensis* hand on the basis of manual proportions and relative thumb length. *J. Hum. Evol.* 2003; 44:225. [PubMed: 12662944]
- Green DJ, Gordon AD. Metacarpal proportions in *Australopithecus africanus*. *J. Hum. Evol.* 2008; 54:705–719. [PubMed: 18191176]
- Rolian C, Gordon AD. Reassessing manual proportions in *Australopithecus afarensis*. *Am. J. Phys. Anthropol.* 2014; 152:393–406. [PubMed: 24104947]
- Bush ME, Lovejoy CO, Johanson DC, Coppens Y. Hominid carpal, metacarpal, and phalangeal bones recovered from the Hadar Formation: 1974–1977 Collections. *Am. J. Phys. Anthropol.* 1982; 57:651–677.
- Ricklan, DE. *From Apes to Angels: Essays in Anthropology in Honor of Phillip V. Tobias*. Sperber, GH., editor. Wiley-Liss; New York: 1990. p. 171–183.

13. Marzke MW, et al. Comparative 3D quantitative analyses of trapeziometacarpal joint surface curvatures among living catarrhines and fossil hominins. *Am. J. Phys. Anthropol.* 2010; 141:38–51. [PubMed: 19544574]
14. Marzke MW, et al. EMG study of hand muscle recruitment during hard hammer percussion manufacture of Oldowan tools. *Am. J. Phys. Anthropol.* 1998; 105:315–332. [PubMed: 9545075]
15. Napier JR. Fossil metacarpals from Swartkrans. *Fossil Mamm. Africa.* 1959; 17:1–18.
16. Susman, RL. Evolutionary History of the “Robust” Australopithecines. Grine, FE., editor. *Aldine de Gruyter*; New York: 1988. p. 149-172.
17. Trinkaus, E. *The Shanidar Neandertals.* Academic Press; London: 1983.
18. Lovejoy CO, Simpson SW, White TD, Asfaw B, Suwa G. Careful climbing in the Miocene: the forelimbs of *Ardipithecus ramidus* and humans are primitive. *Science.* 2009; 326:70e1.
19. Almécija S, Moyà-Solà S, Alba D. Early origin for human-like precision grasping: a comparative study of pollical distal phalanges in fossil hominins. *PLoS One.* 2010; 5:11717. [PubMed: 20661444]
20. Ward CV, Kimbel WH, Harmon EH, Johanson DC. New postcranial fossils of *Australopithecus afarensis* from Hadar, Ethiopia (1990-2007). *J. Hum. Evol.* 2012; 63:1–51. [PubMed: 22652491]
21. Shrewsbury MM, Marzke MW, Linscheid RL, Reece SP. Comparative morphology of the pollical distal phalanx. *Am. J. Phys. Anthropol.* 2003; 121:30–47. [PubMed: 12687581]
22. There are two manual non-pollical distal phalanges from Dmanisi, Georgia<sup>23</sup> associated with *H. erectus*. However, although these phalanges are figured in<sup>23</sup> and appear to also have broad apical tufts like modern humans, these fossils have not yet been described and no metrics are provided. Thus, formal comparisons to *H. erectus* distal phalanges are not yet possible.
23. Lordkipanidze D, et al. Postcranial evidence from early *Homo* from Dmanisi, Georgia. *Nature.* 2007; 449:305–310. [PubMed: 17882214]
24. Lewis, OJ. *Functional morphology of the Evolving Hand and Foot.* Oxford University Press; New York: 1989.
25. Tocheri, MW. Three-dimensional riddles of the radial wrist: derived carpal and carpometacarpal joint morphology in the genus *Homo* and the implications for understanding the evolution of stone tool-related behaviours in hominins. Arizona State Univ.; 2007. PhD thesis
26. Ward CV, Tocheri MW, Plavcan JM, Brown FH, Kyalo Manthi F. Early Pleistocene third metacarpal from Kenya and the evolution of modern human-like hand morphology. *Proc. Natl. Acad. Sci. USA.* 2013; 111:121–124. [PubMed: 24344276]
27. Rolian C, Lieberman DE, Zermeno JP. Hand biomechanics during simulated stone tool use. *J. Hum. Evol.* 2011; 61:26–41. [PubMed: 21420144]
28. Napier JR. Fossil hand bones from Olduvai Gorge. *Nature.* 1962; 196:409–411.
29. McHenry HM. The capitate of *Australopithecus afarensis* and *A. africanus*. *Am. J. Phys. Anthropol.* 1983; 62:187–198. [PubMed: 6418011]
30. Ward CV, et al. South Turkwel: a new Pliocene hominid site in Kenya. *J. Hum. Evol.* 1999; 36:69–95. [PubMed: 9924134]
31. Ward CV, Leakey MG, Walker A. Morphology of *Australopithecus anamensis* from Kanapoi and Allia Bay, Kenya. *J. Hum. Evol.* 2001; 41:255–368. [PubMed: 11599925]
32. Tocheri MW, et al. The primitive wrist of *Homo floresiensis* and its implications for hominin evolution. *Science.* 2007; 317:1743–1745. [PubMed: 17885135]
33. Orr CM, et al. New wrist bones of *Homo floresiensis* from Liang Bua (Flores, Indonesia). *J. Hum. Evol.* 2013; 64:109–129. [PubMed: 23290261]
34. Tocheri MW, Orr CM, Jacofsky MC, Marzke MW. The evolutionary history of the hominin hand since the last common ancestor of *Pan* and *Homo*. *J. Anat.* 2008; 212:544–562. [PubMed: 18380869]
35. Weidenreich F. The extremity bones of *Sinanthropus pekinensis*. *Paleontol. Sinica New Series D.* 1941; 5:1–150.
36. A single modern human outlier in our trapezium sample (n=119) displays a similar combination of even smaller relative articular areas of the Mc1 (10.9%) and scaphoid (5.3%) facets. Thus, while

certainly atypical, relatively small facets like those of the Hand 1 trapezium occasionally occur in modern humans.

37. Marzke MW, Marzke RF. Evolution of the human hand: approaches to acquiring, analyzing and interpreting the anatomical evidence. *J. Anat.* 2000; 197:121–140. [PubMed: 10999274]
38. Deane AS, Begun DR. Broken fingers: retesting locomotor hypotheses for fossil hominoids using fragmentary proximal phalanges and high-resolution polynomial curve fitting (HR-PCF). *J. Hum. Evol.* 2008; 55:691–701. [PubMed: 18692864]
39. Preuschoft, H. The Chimpanzee. Bourne, GH., editor. Vol. 6. Karger; Basel: 1973. p. 34–120.
40. Hunt KD. Mechanical implications of chimpanzee positional behaviour. *Am. J. Phys. Anthropol.* 1991; 86:521–536. [PubMed: 1776659]
41. Jungers WL, Godfrey LR, Simons EL, Chatrath PS. Phalangeal curvature and positional behaviour in extinct sloth lemurs (Primates, Palaeopropithecidae). *Proc. Natl. Acad. Sci.* 1997; 94:11998–12001. [PubMed: 11038588]
42. Richmond BG. Biomechanics of phalangeal curvature. *J. Hum. Evol.* 2007; 53:678–690. [PubMed: 17761213]
43. Deane AS, Kremer EP, Begun DR. A new approach to quantifying anatomical curvatures using High Resolution Polynomial Curve Fitting (HR-PCF). *Am. J. Phys. Anthropol.* 2005; 128:630–638. [PubMed: 15861424]
44. Nguyen NH, Pahr DH, Gross T, Skinner MM, Kivell TL. Micro-finite element (FE) modeling of the siamang (*Symphalangus syndactylus*) third proximal phalanx: The functional role of curvature and the flexor sheath ridge. *J. Hum. Evol.* 2014; 67:60–75. [PubMed: 24496040]
45. Richmond, BG. Ontogeny and Biomechanics of Phalangeal Form in Primates. Stony Brook Univ.; 1998. PhD thesis
46. Marzke MW, Shrewsbury MM, Horner KE. Middle phalanx skeletal morphology in the hand: Can it predict flexor tendon size and attachments? *Am. J. Phys. Anthropol.* 2007; 134:141–141. [PubMed: 17568442]
47. Ward CV. Interpreting the posture and locomotion of *Australopithecus afarensis*: Where do we stand? *Yrbk. Phys. Anthropol.* 2002; 45:185–215. [PubMed: 12653313]
48. Latimer, B. Origine(s) de la bipédie chez les Hominidés. Senut, B.; Coppens, Y., editors. CNRS; Paris: 1991. p. 169–176.
49. Tuttle RH. Evolution of hominid bipedalism and prehensile capabilities. *Phil. Trans. Royal Soc. London B.* 1981; 292:89–94.
50. Stern JT Jr, Susman RL. The locomotor anatomy of *Australopithecus afarensis*. *Am. J. Phys. Anthropol.* 1983; 60:279–317. [PubMed: 6405621]
51. Lieberman DE. Making behavioural and phylogenetic inferences from hominid fossils: Considering the developmental influence of mechanical forces. *Annu. Rev. Anthropol.* 1997; 26:185–210.
52. Harcourt-Smith WEH, et al. The foot of *Homo naledi*. *Nat. Commun.* this issue.
53. Smith SL. Shape variation of the human pollical distal phalanx and metacarpal. *Am. J. Phys. Anthropol.* 2000; 113:329–348. [PubMed: 11042536]
54. Tocheri MW, et al. Ecological divergence and medial cuneiform morphology in gorillas. *J. Hum. Evol.* 2011; 60:171–184. [PubMed: 21093014]
55. Mosimann JE. Size allometry: size and shape variables with characterizations of the log-normal and gamma distributions. *J. Am. Stat. Assoc.* 1970; 56:930–945.
56. Falsetti AB, Jungers WL, Cole TMI. Morphometrics of the callitrichid forelimb: a case study of size and shape. *Int. J. Primatol.* 1993; 14:551–571.
57. Jungers WL, Falsetti AB, Wall CE. Shape, relative size, and size-adjustments in morphometrics. *Yrbk. Phys. Anthropol.* 1995; 38:137–161.
58. Tocheri MW, et al. Functional capabilities of modern and fossil hominid hands: three-dimensional analysis of the trapezia. *Am. J. Phys. Anthropol.* 2003; 122:101–112. [PubMed: 12949830]
59. Tocheri MW, Razdan A, Williams RC, Marzke MW. A 3D quantitative comparison of trapezium and trapezoid relative articular and non-articular surface areas in modern humans and great apes. *J. Hum. Evol.* 49:570–586. [PubMed: 16085278]

60. Deane AS, Kremer EP. 3D or not to 3D, A comment on De Groote et al. *Am. J. Phys. Anthropol.* 2010; 143:638–639. 2010. [PubMed: 20872804]



**Figure 1. *H. naledi* Hand 1 adult right hand**

(A) Palmar (left) and dorsal (right) views of the right hand bones, (B) found *in situ* in semi-articulation with the palm up and fingers flexed. The palmar surface of the metacarpals (Mc) and dorsal surface of the intermediate phalanges (IP) can be seen. ‘PP’, proximal phalanx; ‘DP’, distal phalanx.

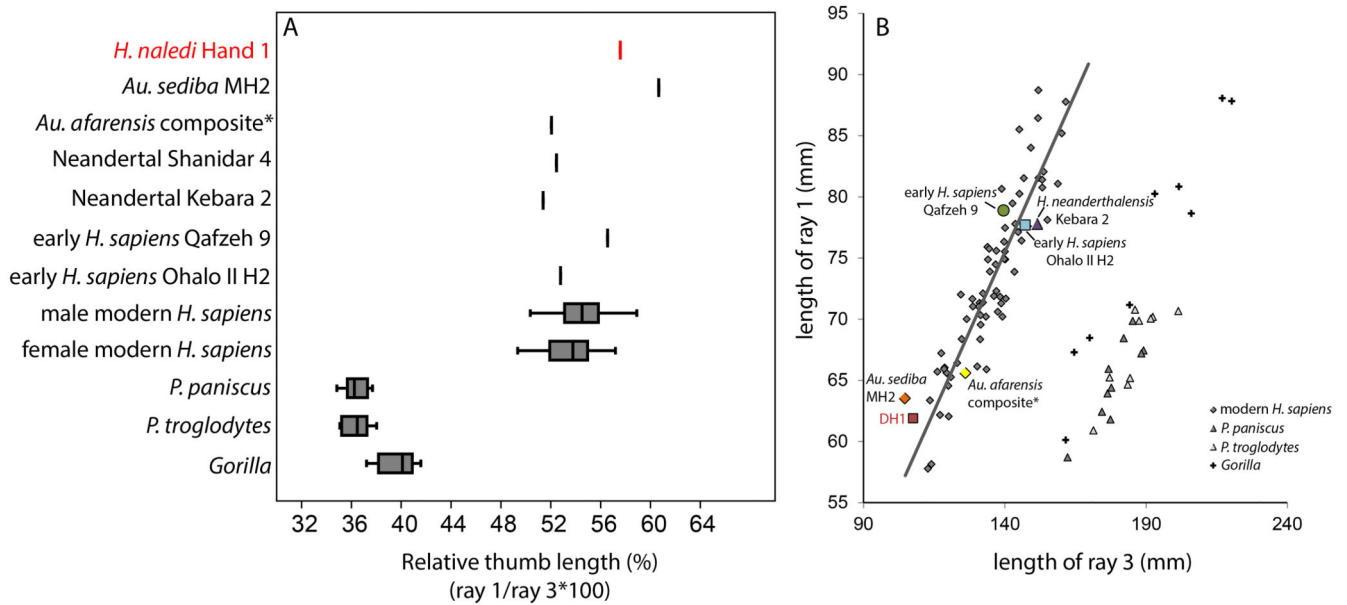


**Figure 2. Relative length of the thumb in *H. naledi* Hand 1**

Relative length of the thumb (ray 1, total length of the first metacarpal and first proximal phalanx) and third ray (total length of the third metacarpal and third proximal and intermediate phalanges) within the same individual, in all taxa except *Au. afarensis* (\*), for which the ratio is one potential estimate of hand proportions derived from multiple individuals<sup>7,8,10</sup>. (A) A box-and-whisker plot, where the box represents the 25th and 75th percentiles, the centre line represents the median, and the whiskers represent the non-outlier range, of ray 1 to ray 3 length (as a percentage) demonstrates that Hand 1 has a relatively longer thumb than all other hominins, apart from *Au. sediba*, and falls within the upper range of variation in modern human males only. (B) Linear regression of ray 1 length to ray 3 length, with regression line fit to modern humans (males and females combined), shows that Hand 1 has a relatively long thumb for its small hand size, falling on the edge of modern human variation. Male and female modern humans sample comprises African (n=31), Nubian Egyptian (n=11) and small-bodied Khoisan (n=25) individuals. Data for Shanidar 4 is derived from<sup>19</sup>.

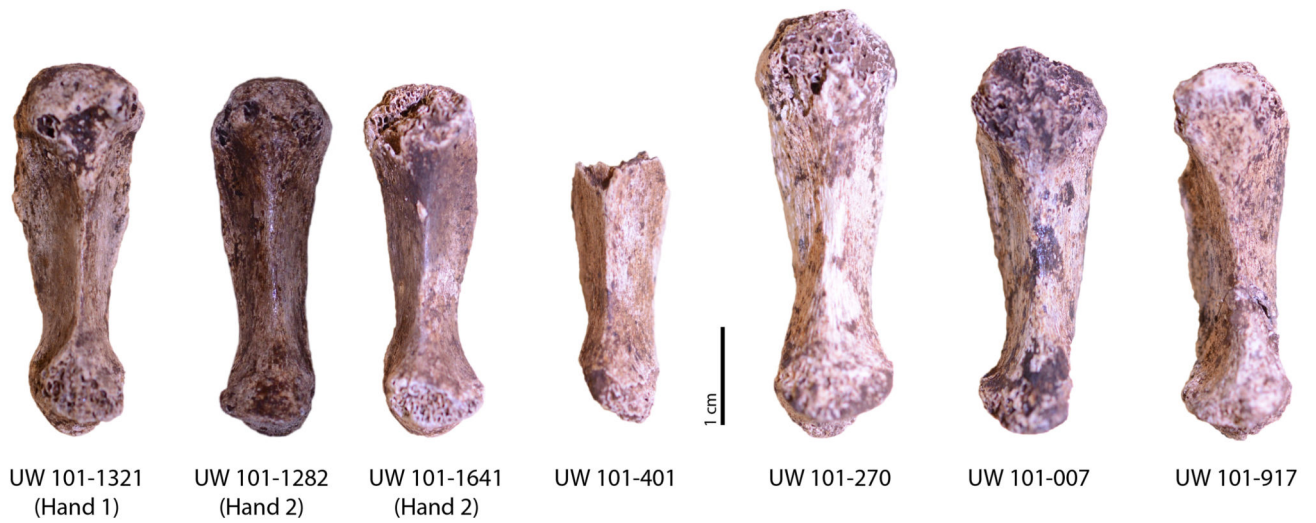


**Figure 3. *H. naledi* pollical metacarpal (Mc1) morphology**

Palmar view of the current sample of *H. naledi* Mc1s, including the right Mc1 of Hand 1, left and right Mc1 associated with a second individual (Hand 2), and four isolated Mc1s from four other individuals, demonstrating the homogeneity of *H. naledi* Mc1 morphology and variation in size across the sample.

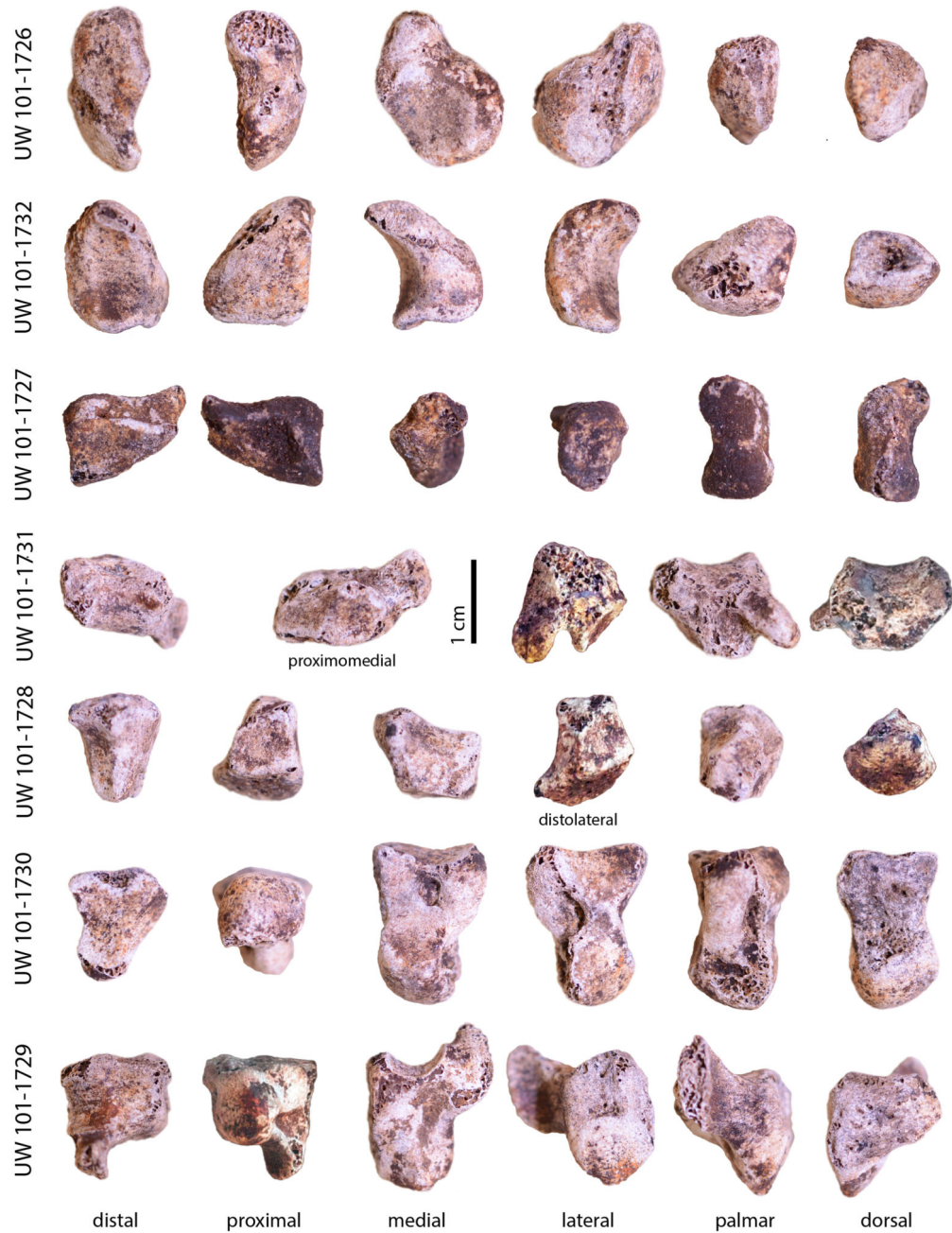


**Figure 4. *H. naledi* Hand 1 wrist bones**

The associated carpal bones of Hand 1, showing (from top to bottom), the scaphoid, lunate, triquetrum, trapezium, trapezoid, capitate and hamate in standard anatomical views. The trapezium is shown in proximomedial view to depict the trapezoid and scaphoid facets, and the trapezoid is shown in distolateral view to demonstrate the distinctive modern human-like “boot-shape”. All bones to scale.



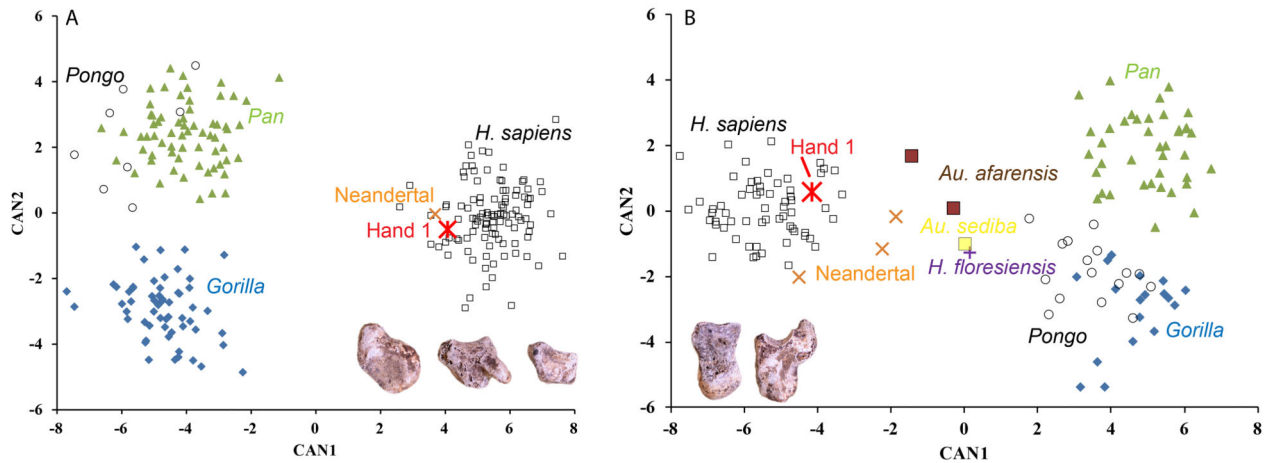


**Figure 5. Three-dimensional multivariate analysis of *H. naledi* wrist bone shape**

The first (CAN1) and second (CAN2) canonical variates of the (A) scaphoid, trapezium and trapezoid (STT, inset image) combined, including 15 angles, 13 relative areas and two curvatures, and (B) the capitate and hamate (CH, inset image) combined, including 12 angles, nine relative areas and four other hamate metrics. In the STT analysis, CAN1 and CAN2 explain 79.6% and 12.7% of the variance, respectively and in the CH analysis, CAN1 explains 84.8% and CAN2 8.9%, respectively. Fossil elements were analyzed as test classification cases only and do not contribute to the observed variation along the canonical axes. In all cases, the posterior probabilities classify the Hand 1 (and Neandertal) wrist bones as 100% *H. sapiens*, compared with *Au. afarensis* AL 333 classified as *H. sapiens* (50%) and *Pongo* (50%), *Au. sediba* as *Gorilla* (52%) and *Pongo* (39%) and *H. floresiensis* as *Gorilla* (62%) and *Pongo* (36%).

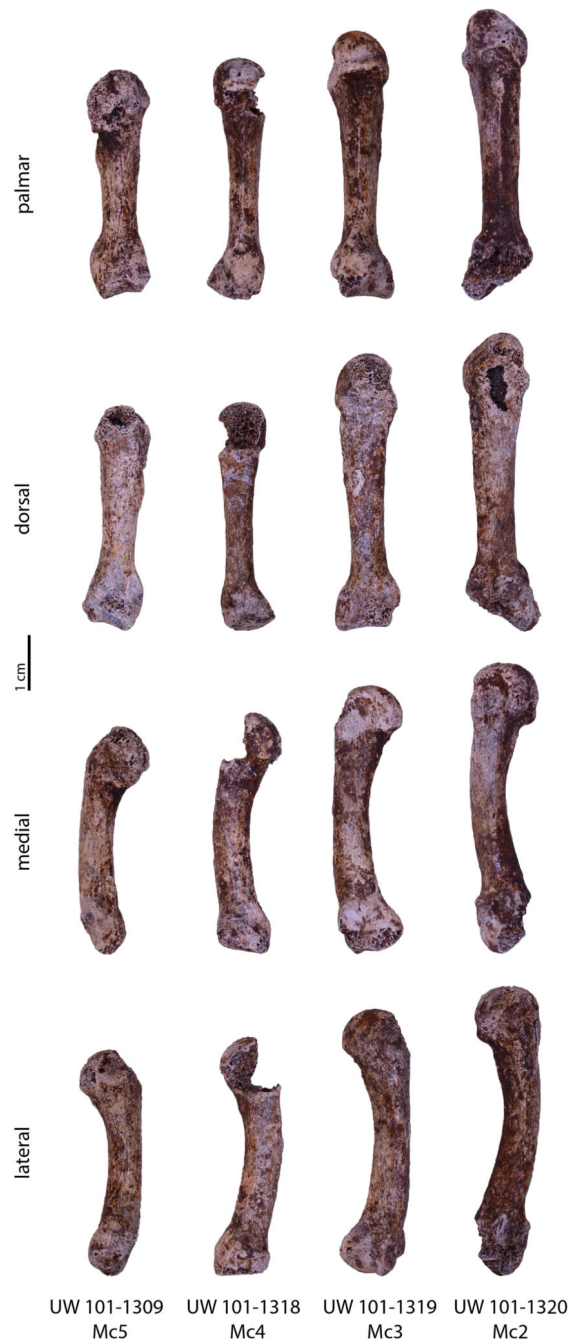


**Figure 6. *H. naledi* Hand 1 non-pollical metacarpals**

The associated medial metacarpals (Mc) of Hand 1 hand in standard anatomical views. Note the absence of the styloid process from the proximal base of the Mc3 and general robusticity of all the metacarpals, particularly Mc5.

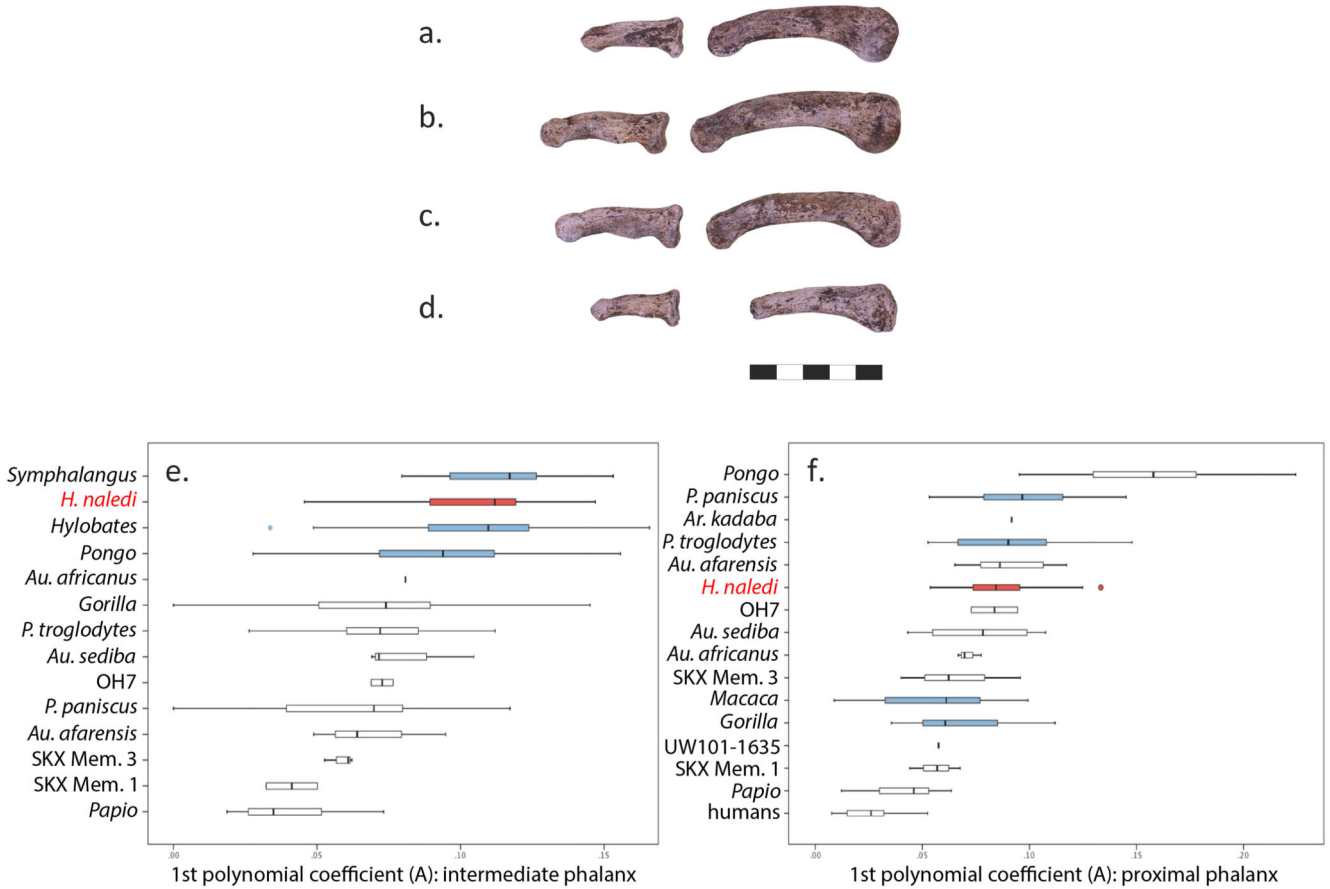


**Figure 7. Phalangeal curvature in *H. naledi***

Above, proximal and intermediate phalanges of the Hand 1 (a) second, (b) third (c) fourth and (d) fifth ray in lateral view (all to scale). Below, box-and-whisker plots of curvature in *H. naledi* (e) intermediate phalanges (n=14) and (f) proximal phalanges (n=11), quantified as the 1<sup>st</sup> polynomial coefficient (A) of the polynomial functions ( $y=Ax^2+Bx+C$ ) representing longitudinal shaft curvature of the dorsal surface. Vertical line represents the median value, boxes show the interquartile range, and whiskers extend to the highest and lowest values of each taxon, excluding outliers (dots). The *H. naledi* sample is shown in red and extant taxa that are not statistically distinct from this sample (p 0.05 based on one-way ANOVA with Bonferroni correction) are shown in blue. “SKX Mem. 1” and “SKX Mem. 3” refer to the Swartkans phalanx sample from Members 1 and 3, respectively that can be attributed to either *Au. robustus* or early *Homo*. ‘UW 101-1635’ is a juvenile *H. naledi* proximal phalanx. *H. naledi* is unusual compared to most other hominins in having both strongly curved proximal and intermediate phalanges.